Raman investigation of rotational and translational excitations in K1−x (NH4) x I mixed crystals

J.F. Berret, J.L. Sauvajol, and S. Haussühl

Citation: The Journal of Chemical Physics **96**, 4896 (1992); doi: 10.1063/1.462779
View online: http://dx.doi.org/10.1063/1.462779
View Table of Contents: http://scitation.aip.org/content/aip/journal/jcp/96/7?ver=pdfcov
Published by the AIP Publishing

Raman investigation of rotational and translational excitations in $K_{1-x}(NH_4)_xI$ mixed crystals

J.-F. Berret
Laboratoire de Sciences des Matériaux Vitreux, U.A. CNRS 1119, Université de Montpellier II, F-34095 Montpellier, France

J.-L. Sauvajol
Groupe de Dynamique des Phases Condensées, U.A. CNRS 233, Université de Montpellier II, F-34095 Montpellier, France

S. Haussühl
Institut für Kristallographie der Universität zu Köln, D-5000 Köln, Germany

(Received 7 October 1991; accepted 20 December 1991)

Using Raman scattering experiments we have investigated the rotational and translational modes in $K_{1-x}(NH_4)_xI$ mixed crystals for ammonium concentrations $x = 0.005$, 0.07, 0.16, and $x = 0.46$ and in a fully deuterated isomorph with $x(D) = 0.42$. The $A_{1g} + 4E_g$ and T_{2g} Raman responses have been measured at atmospheric pressure in the paraelectric plastic phase ($T = 295$ K) and in the orientational glassy phase ($T = 7$ K). In the low-frequency region $\nu = 5$–$600\ cm^{-1}$, seven Raman active components could be identified. These bands are entirely due to the admixture of anisotropic NH_4^+ to pure KI. Their contributions result either from reorientations of the molecules between equivalent directions and rotational-like excitations around these preferential orientations, or from translational modes of the whole Brillouin zone. In this peculiar case, orientational disorder of the ammonium lifts wave vector conservation of the scattering processes. An interpretation of the different Raman allowed transitions is proposed. The composition and polarization dependences as well as the effect of deuteration for these modes are discussed with respect to earlier reports.

I. INTRODUCTION

Ammonium halides are well known to undergo numerous structural modifications under cooling.[1] Recently, in ammonium iodide, it has been shown that a substitution of the slightly anisotropic NH_4^+ tetrahedra by spherical K^+ ions suppresses these transitions.[2–7] The mixed crystals derived from this random substitution, $K_{1-x}(NH_4)_xI$, have attracted increasing interest, since they exhibit a low-temperature orientational glass phase devoid of long range order.[4] The orientational degrees of freedom involved in the disordered frozen state are related to induced electric dipoles associated to the ammonium tetrahedra.[4,6]

KI:NH_4I mixed systems are in a NaCl rock salt structure ($Fm3m$) at room temperature. This phase is characterized by a dynamical disorder of the NH_4^+ molecules. It is now established that fast molecular orientations take place in the octahedral crystal field of symmetry C_{3v}, yielding for the molecule eight equivalent orientations along the $\langle 111 \rangle$ crystalline axes.[8] Within this picture, one N–H bond points toward the cube diagonals, whereas the other three bonds tend toward the neighboring iodide ions. This is the so-called "triple-approach model." From this nonequivalence of the N–H bonds, a deformation of the tetrahedra occurs, which accounts for the large dipolar moment revealed by dielectric experiments.[4] This microscopic picture for the site symmetry of the ammoniums will be assumed to be valid over the whole composition range.

We report in this paper a low-frequency Raman scattering investigation of the mixed $K_{1-x}(NH_4)_xI$ single crystals and their deuterated isomorphs for NH_4^+ (or ND_4^+) compositions ranging from 0.5% to 46%. Raman spectra have been measured at atmospheric pressure in the low-frequency region $\nu = 5$–$600\ cm^{-1}$, in the paraelectric plastic phase at room temperature and in the glassy phase at $T = 7$ K.

Our purpose was twofold: rotational excitations of NH_4^+ incorporated in alkali halides at low concentrations (i.e., a few percent) have been evidenced by means of incoherent inelastic neutron scattering (INS).[9,10] These rotational excitations connected to the NH_4^+ dynamics (due to reorientations, librations, torsions of the molecules, etc.) should also contribute to the Raman response. As a second motivation, there is the well-known property that for molecular crystals orientational disorder lifts the wave vector conservation of the scattering processes, and thus phonons of the whole Brillouin zone contribute to the light scattering spectrum. This has been established in the different phases of NH_4I.[11–13] Since phonons are expected to play a crucial role in the orientational glass transition,[3,6] it is a question of interest to check if translational modes can also be detected by Raman scattering. The study of five concentrations in NH_4I should finally allow us to follow the variation of rotational and translational modes from the dilute limit ($x < 10\%$) into the orientational glass ($x \simeq 0.5$). The comparison of protonated and deuterated samples with comparable composition [$x(D) = 0.42$ and $x = 0.46$] should also allow us to check the effects of deuteration on the dynamical modes.

 0021-9606/92/074896-08$06.00

The outline of the paper is as follows: Experimental details and results are presented in the Sec. II. In Sec. III, an interpretation of the Raman allowed transitions is proposed and the composition dependences of these bands at ambient and low temperatures are discussed with respect to earlier results. Final conclusions are drawn in Sec. IV.

II. EXPERIMENTAL TECHNIQUES AND RESULTS

$K_{1-x}(NH_4)_xI$ single crystals with $x = 0.005$ 0.07, 0.16, 0.42 (D), and 0.46 were all grown from aqueous solutions (the suffix (D) in parentheses refers to a fully deuterated compound). Their ammonium concentrations were determined by measuring the mass fraction of nitrogen atoms from small pieces. As illustrated in Table I, the NH_4I concentration in the solution and the true concentration differ significantly, a usual property for molecular mixed crystals.[14] The protonated mixtures with $x = 0.16$ and $x = 0.46$ and the deuterated one with $x(D) = 0.42$ originate from the same batch as the samples studied in Ref. 3 and Ref. 6, respectively.

Raman spectra were recorded using a "Coderg T800" triple monochromator with a resolution between 0.65 and 1.5 cm^{-1} (half-width at half-maximum—HWHM—of the instrumental linewidth), depending on the temperature range. 300 mW of an Ar^+-ion laser working at $\nu_0 = 514.5$ nm were focused on freshly cleaved monocrystals in a 90° configuration, the incident and scattered wave vectors propagating along the $x = \langle 100 \rangle$ and $y = \langle 010 \rangle$ crystalline directions, respectively. Both VV $[x(zz)y]$ and VH $[x(zx)y]$ polarization spectra for the frequency range $\nu = 0$–600 cm^{-1} were measured, corresponding for cubic crystals to Raman-allowed transitions of $A_{1g} + 4E_g$ and T_{2g} symmetries, respectively.

A. Room temperature Raman spectra

Figures 1 and 2 display the spectral evolution of the Raman response for mixed crystals at $x = 0.005$, 0.07, 0.16, 0.42 (D), and $x = 0.46$ in the low-frequency region $\nu \leqslant 250$ cm^{-1} for $A_{1g} + 4E_g$ and T_{2g} scattering geometries, respectively. As the concentration increases (Fig. 1), a double peak emerges at 50–60 cm^{-1}, which broadens to become an asymmetric feature at $x = 0.46$. The $[x(zz)y]$ spectra at intermediate x resemble that of pure NH_4I first reported by Dultz and Ihlefeld.[11] It should be noticed that the relatively weak scattering intensity of the deuterated sample at $x(D) = 0.42$ compared to the similarly substituted compound ($x = 0.46$) is mainly due to the poor optical quality of the crystal.

TABLE I. List of the molar concentrations x as given in the aqueous solution and as measured for the $K_{1-x}(NH_4)_xI$ mixed crystals investigated here.

NH_4I concentration in the solution (%)	NH_4^+ concentration measured (%)
1	0.5
10	7
20	16 ± 1
50 (D)	42 ± 1
50	46 ± 2

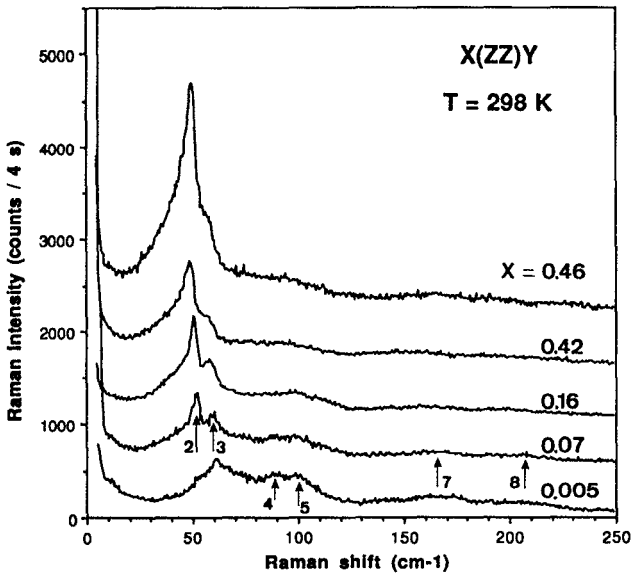

FIG. 1. Low-frequency Raman spectrum of $K_{1-x}(NH_4)_xI$ at room temperature ($T = 298$ K) observed in the $[x(zz)y]$ scattering geometry (symmetry $A_{1g} + 4E_g$). The spectra for $x = 0.07$, 0.16, 0.46, and for the fully deuterated crystal with $x(D) = 0.42$ have been shifted with respect to each other for sake of clarity. Arrows indicate the Raman components described in the text. The intensity for the $x = 0.46$ sample has been divided by a factor 2.

A closer inspection of the $[x(zz)y]$ and $[x(zx)y]$ data reveals the presence of seven main lines below 250 cm^{-1}, labeled with increasing frequency ν_1 to ν_8 (ν_6 is only observable at low temperatures). These transitions are indicated by arrows in Figs. 1 and 2. Bands ν_1–ν_5 show up in spectra from

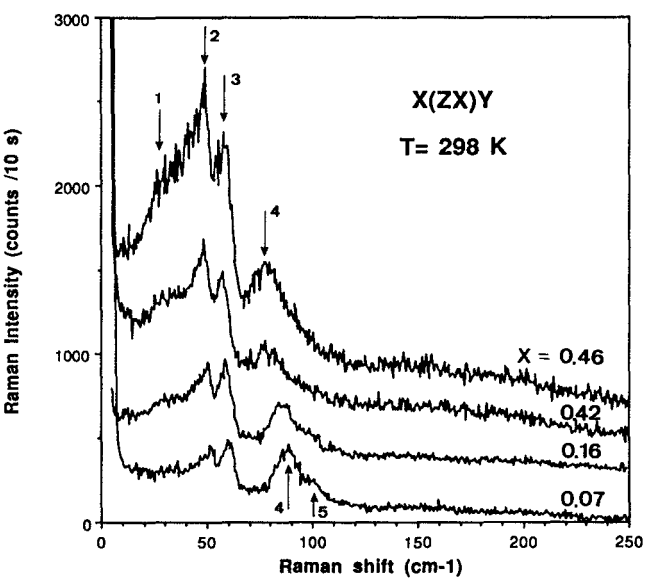

FIG. 2. As in Fig. 1 but for the $[x(zy)z]$ scattering geometry (symmetry T_{2g}).

TABLE II. Compilation of the frequencies (in cm^{-1}) for the most prominent Raman active components shown in Figs. 1 and 2.

Band #	Polarization	0.5% H	7% H	16% H	42% D	46% H
2	VV/VH	51.8(±0.2)	51.9(±0.2)	50.9(±0.2)	48.5(±0.2)	49.5(±0.2)
3	VV/VH	61.3(±0.1)	60.0(±0.2)	58.9(±0.3)	57.5(±0.3)	58.7(±0.3)
4	VV/VH	···	88.3(±0.2)	86 (±0.5)	79 (±1)	78 (±1)
7	VV	167 (±2)	165 (±2)	157 (±2)	151 (±2)	163 (±2)
8	VV	208 (±2)	207 (±1)	199 (±2)	187 (±3)	196 (±4)

both scattering geometries, whereas the two other lines ν_7 and ν_8 at higher energy appear only in the $[x(zz)y]$ polarization spectra.

Except for ν_1 at low x and ν_5 at intermediate x, the features described above are present at all concentrations. However, an overall broadening of these bands is observed as x varies from 0.5% to 46%. The frequency shifts for the most prominent ones, i.e., $\nu_2-\nu_4$ and $\nu_7-\nu_8$, as well as the accuracy in their determination, are listed in Table II. The nature of all these Raman features will be specified in the next section (except for ν_5 which cannot be followed with concentration change).

B. Low temperature Raman spectra

The five mixed crystals used in our experiment remain transparent at low temperature, suggesting that the f.c.c. cubic structure is stabilized.[2-7] In pure ammonium iodide, the NaCl→CsCl transformation is accompanied by a loss of transparency of the crystal.[3]

The aperture width of the spectrometer was enhanced for the measurements at low temperature in order to augment the signal-to-noise ratio. Figure 3 shows the evolution of the Raman response in mixed ammonium/potassium iodide crystals ($x = 0.46$) from the plastic phase ($T = 295$ K) to the orientational glassy state ($T = 7$ K). The relative intensity at each temperature can be compared, since the scattered light is plotted for the same counting time, $t = 5$ s. As a consequence of temperature change, the features reported in Fig. 1 are now much narrower and better defined, and some of them have larger magnitudes.

In Figs. 4 and 5, a representation of the low-temperature Raman responses equivalent to that of Figs. 1 and 2 was used. Here, as in Fig. 3, six main lines (shown by arrows) can be distinguished below 250 cm^{-1}. Compared to the results of Figs. 1 and 2, these lines all show up in both polarizations, this effect being most remarkable in $K_{0.54}(NH_4)_{0.46}I$. Only ν_4 and ν_5 do not seem to have low-temperature counterparts (except possibly the weak line observed in Fig. 5 around 80 cm^{-1}, for $x = 0.07$).

The temperature effect on the lines present in both plastic and frozen states can be estimated in Table III where $\nu_1-\nu_3$ and $\nu_6-\nu_8$ are compiled with their accuracy. In Figs. 6

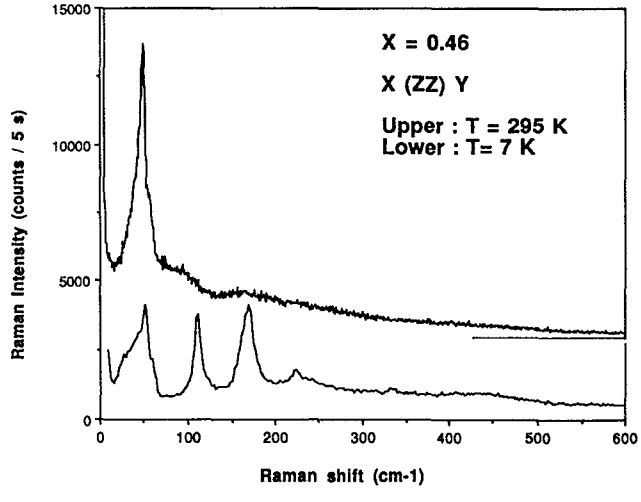

FIG. 3. Evolution of the $A_{1g} + 4E_g$ Raman response in $K_{0.54}(NH_4)_{0.46}I$ between the room temperature plastic phase ($T = 295$ K, upper spectrum) and the low-temperature orientational glass state ($T = 7$ K, lower spectrum). The HWHM of the instrumental linewidth are 0.65 and 1.5 cm^{-1}, respectively. The data have been shifted for sake of clarity.

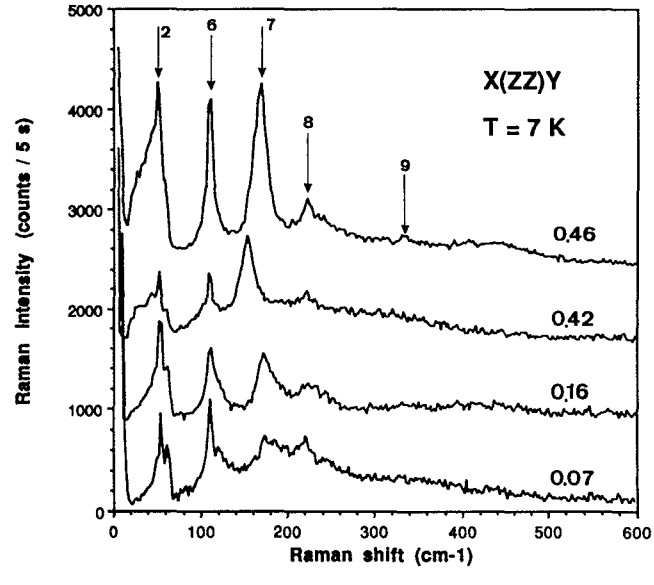

FIG. 4. Low-frequency Raman spectrum of $K_{1-x}(NH_4)_xI$ at $T = 7$ K observed in the $[x(zz)y]$ scattering geometry (symmetry $A_{1g} + 4E_g$). The spectra for $x = 0.16$, 0.46, and for the fully deuterated crystal with $x(D) = 0.42$ have been shifted with respect to each other. Arrows refer to the same Raman components defined in Figs. 1 and 2 (see the text). The intensity for the $x = 0.46$ sample has been divided by a factor 2.

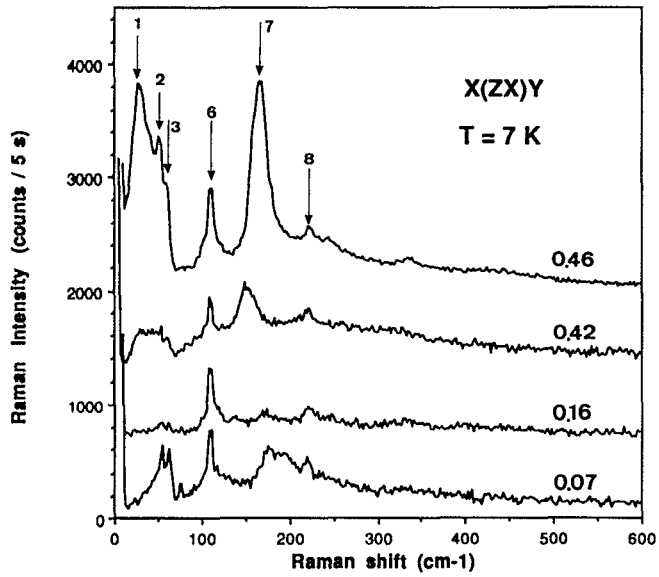

FIG. 5. As in Fig. 4 but for the $[x(zy)z]$ scattering geometry (symmetry T_{2g}).

and 7 are displayed the band positions given above for room temperature and $T = 7$ K, respectively.

III. INTERPRETATION

In a completely ordered cubic crystal, the first order Raman cross section should be zero. The Raman active components of $K_{1-x}(NH_4)_xI$ described before are thus entirely due to the admixture of anisotropic NH_4^+ to pure KI. Their contributions result either directly from reorientations of the molecules between equivalent directions and rotational-like excitations around these preferential orientations, or indirectly from translational modes of the whole Brillouin zone. In this last case, orientational disorder of the ammonium lifts wave vector conservation of the scattering processes. These three types of scattering events are indeed observed in $K_{1-x}(NH_4)_xI$ and will be treated separately in the following subsections.

A. Quasielastic scattering

In Figs. 1 and 2 and more obviously in Fig. 3, in the range 300–600 cm^{-1} the decreasing of the overall Raman intensity with increasing ν attests to the presence of a quasielastic component. This contribution of the NH_4^+ reorientations to the scattered light spectrum shows up even at low compositions and in both polarizations. In molecular crystals, it is usually approximated by a Lorentzian function whose width is connected to the reorientational mean time of the molecules.

In the present case, however, the low-energy features of $K_{1-x}(NH_4)_xI$ observed below 250 cm^{-1} prevent any quantitative determination of this central component. Only a qualitative approach can be provided: First, the fact that NH_4^+ reorientations contribute in both scattering geometries ($A_{1g} + 4E_g$ for Fig. 1 and T_{2g} for Fig. 2) is in agreement with the triple-approach model of ⟨111⟩ preferential orientations.[15] Second, the quasielastic component is practically x independent and vanishes totally at 7 K (see Fig. 3). This last property is consistent with the assumption of frozen-in reorientations at low temperatures.

Finally, these findings confirm the earlier Raman report on phase I of NH_4I (Ref. 11). A quasielastic central peak with an HWHM of 30 cm^{-1} at room temperature was proposed, a value compatible with the present data.

B. Phonon density of states

1. Acoustic modes

$A_{1g} + 4E_g$ and T_{2g} spectra up to 70 cm^{-1} are due to the density of states of acoustic phonons. An analogous conclusion was already drawn by Dultz and Ihlefeld in phase I of pure ammonium iodide.[11] More insight in the assignment of ν_1–ν_3 can be gained by comparing the present spectra with recent and still unpublished results obtained by coherent inelastic neutron scattering.[16] We have measured the dispersion curves for translational modes propagating in the high-symmetry directions of the mixed $K_{0.58}(ND_4)_{0.42}I$ single crystal at room temperature. From these curves we are able to deduce the frequencies at which the phonon density of states passes through maxima, i.e., where the slope $\partial\nu(q)/\partial q$ tends to zero. These frequencies and their assignments are indicated as arrows in Fig. 8. Here the Raman intensities at $x(D) = 42\%$ are plotted for $[x(zz)y]$ and $[x(zx)y]$ polarizations in an extended scale compared to Fig. 1. We hence assign the main component ν_2 to transverse phonons propagating along the [110] direction, whereas ν_3 arises from the longitudinal phonons traveling along the [100] axis. On the other hand, ν_1 coincides with the frequency of zone bound-

TABLE III. As in Table II, but for the Raman features observed at low temperature ($T = 7$ K, see Figs. 3 and 4).

Band #	Polarization	7% H	16% H	42% D	46% H
1	VV/VH	n.o.	30.7(±0.5)	29.3(±0.5)	28.5(±0.2)
2	VV/VH	54.6(±0.2)	54.4(±0.3)	51.7(±0.3)	53.2(±0.3)
3	VV/VH	63.2(±0.2)	62.3(±0.5)	61.0(±0.5)	60 (±1)
6	VV/VH	109.9(±2)	110.5(±2)	110.0(±2)	110.9(±2)
7	VV/VH	177 (±1)	171.0(±2)	152.6(±3)	169.0
8	VV/VH	218.5(±1)	221 (±1)	220 (±2)	224 (±2)

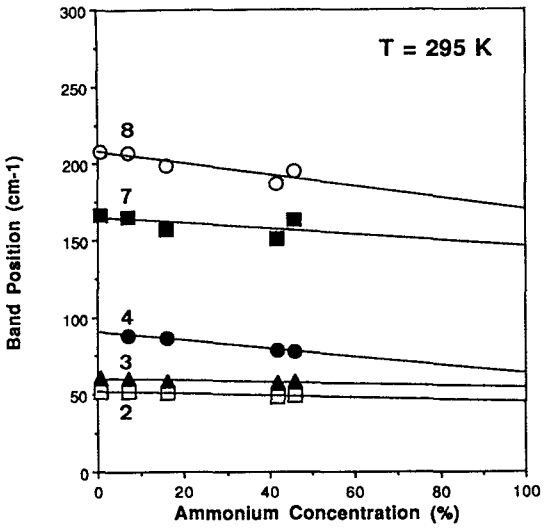

FIG. 6. Variation of the band positions for the most prominent Raman components of Figs. 1 and 2, i.e., $\nu_2-\nu_4$ and $\nu_7-\nu_8$ as functions of the ammonium composition ($T = 295$ K). Straight lines are results of linear regression calculations.

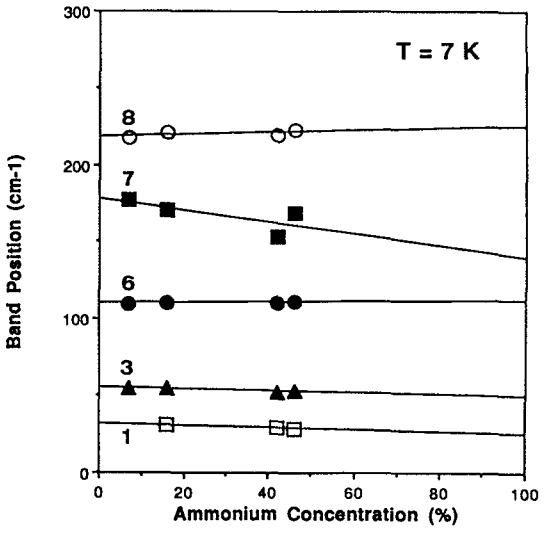

FIG. 7. As in Fig. 6 but for the low-temperature bands ν_1, ν_3, ν_6, ν_7, and ν_8 of Figs. 4 and 5.

ary transverse phonons at the X point. Since this line is only to be seen in concentrated samples [$x(D) = 0.42$ and $x = 0.46$] at low temperatures, it is probably related to the onset of antiferroelectric ordering, as suggested by elastic neutron scattering results.[6]

2. Optical modes

Unfortunately, using the same neutron experiment which permits the measurement of the acoustic branches of $K_{0.58}(ND_4)_{0.42}I$, optical translational modes could not be observed. Hence, in order to identify the nature of the Raman lines at frequency higher than 70 cm^{-1}, we have applied a simple but general concept derived for phonons in ionic mixed crystals by Genzel and Bauhofer[17] (hereafter referred to as GB). For cubic systems of the type $AB_{1-x}C_x$, these authors provided qualitative information concerning the phonon behavior as functions of composition x and wave vector $\mathbf{q}$ on the whole Brillouin zone. The principal foundations of GB's concept are based on (i) the knowledge of the phonon energies at the end-member crystals $x = 0$ and $x = 1$; (ii) the emergence of impurity modes (IM) due to the B↔C substitution approaching $x = 0$ and $x = 1$. Ac-

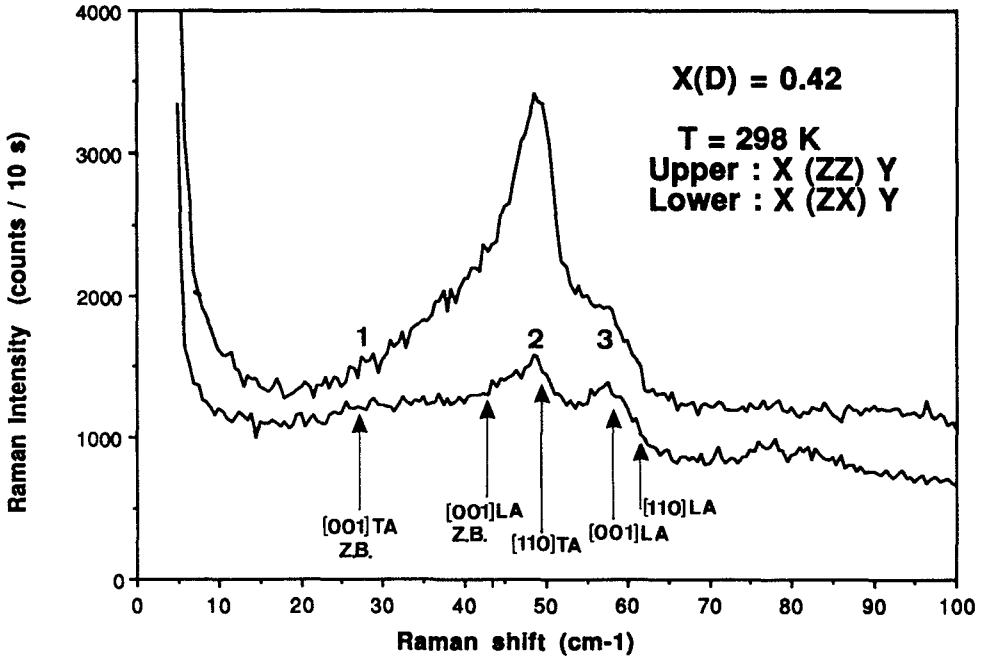

FIG. 8. $A_{1g} + 4E_g$ and T_{2g} Raman spectra for $K_{0.58}(ND_4)_{0.42}I$ at low frequency. The data have been plotted on extended scale ($\nu < 100$ cm^{-1}) compared to Figs. 1 and 2 in order to emphasize the correspondence between the translational modes measured by coherent inelastic neutron scattering (indicated by arrows) (Ref. 16) and the Raman features $\nu_1-\nu_3$ (see the text).

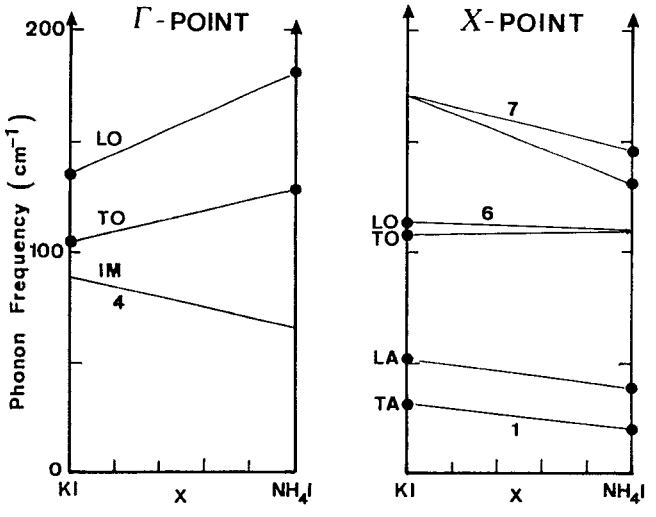

FIG. 9. Schematic concentration dependences of optical phonon modes in $K_{1-x}(NH_4)_xI$ mixed crystals as deduced from Genzel and Bauhofer's model (Ref. 17) (a) for long wavelength phonon at the Γ point; (b) for Brillouin zone boundary phonon at the X point. Room temperature data for longitudinal (LO) and transverse (TO) optical phonons in pure KI and ND_4I (closed circles) are taken from infrared reflectivity (Ref. 18) and neutron scattering works (Refs. 19 and 20). IM stands for impurity mode.

cording to GB, we distinguish for $K_{1-x}(NH_4)_xI$ two kinds of mode behavior, one at the zone center (Γ point) and one at the zone boundary (X or L points). Data for optical bands in KI and ND_4I are taken from infrared reflectivity[18] and neutron scattering studies.[19,20]

a. Zone center mode behavior. Transverse and longitudinal Γ-point phonons for KI are located at 103.5 and 135 cm^{-1} (Ref. 18), respectively, and for ND_4I at 128 and ~180 cm^{-1} (Ref. 20). Then, graphs similar to those proposed by GB can be constructed using these data. The assignment of ν_4 to the impurity mode of NH_4^+ diluted in the KI matrix is then compatible with the so-called one mode behavior, described as Type 3 in GB's formalism. This normal mode behavior is characterized by LO and TO phonons, which go smoothly from one end-member to the other, as illustrated in Fig. 9(a). This assignment is, moreover, the only one able to account for the appearance of a Raman active component ν_4 falling in the gap between acoustic and optical modes.

b. Zone boundary mode behavior. A similar reasoning can be carried out for zone boundary phonons. To this aim, transverse and longitudinal frequencies at the X point are used for KI (at 109 and 113 cm^{-1})[19] and for ND_4I (at 132 and 145 cm^{-1}).[20] Note that the KI data are given for $T = 80$ K. The classification of the different type mode behavior is straightforward, since in the case of zone boundary phonons the atomic masses determine directly the composition dependences. The atomic mass of the iodide ion being much larger than that of both other substitutional elements ($M_I = 126.90u > M_{NH_4} = 18.04u$; $M_K = 39.09u$), $K_{1-x}(NH_4)_xI$ belongs to Type I mode behavior according to GB's classification. In Type I, LO–TO branches of KI merge to the impurity mode due to K^+ in NH_4I crystal, and conversely for NH_4I. This feature is shown in Fig. 9(b). We hence can ascribe ν_6 at 110 cm^{-1} as resulting from the neighboring LO and TO modes of KI. Similarly, ν_7 (~170 cm^{-1}) can be interpreted in terms of an NH_4^+-impurity mode in potassium iodide [see Fig. 9(b)]. For the latter component, the value of the frequency ratio between the protonated (at $x = 0.46$) and its deuterated isomorph [$x(D) = 0.42$] fully confirms the above assignment. The isotopic effect predicts a variation

$$\nu_7(NH_4^+)/\nu_7(ND_4^+) \propto \{m(ND_4^+)/m(NH_4^+)\}^{1/2} = 1.10.$$

At ambient and low temperatures one gets for this frequency ratio 1.08 (Table II) and 1.10 (Table III), respectively.

As far as the optical modes are concerned, it has to be kept in mind, however, that the previous reasoning is qualitative and that Figs. 9(a) and 9(b) are only schematic diagrams. Moreover, for all the lines discussed above, i.e., ν_4, ν_6, and ν_7, their contributions to the Raman spectra are most likely phonon densities of states.

Our analysis is corroborated by incoherent inelastic neutron scattering results obtained from ammonium ions incorporated into alkali halide crystals.[9] In KI containing 4.5% of NH_4^+, Gardner *et al.* reported the existence of three main peaks at 171, 230, and 330 cm^{-1} (for $T = 80$ K). INS measure the density of states of localized excitations of the NH_4^+ ions, which solely contribute to the scattering process (because of the large cross section of the hydrogen atoms). These authors attribute the first band at 171 cm^{-1} to NH_4^+-localized translation modes. This value is in excellent agreement with the Raman data and corresponds to the impurity mode ν_7. For our $x = 7\%$ crystal (the sample with the closest ammonium content compared to that of the INS work), the band energy is found to increase from 165 to 177 cm^{-1} between room temperature and 7 K. Note finally that the INS feature reported at 330 cm^{-1} (Ref. 9) is also Raman active and may correspond to the weak line ν_9 displayed in Fig. 4.

C. Rotational excitations of NH_4^+ molecules

The last Raman active mode discussed in this work, ν_8, originates from librational motions about the C_3 symmetry axis. ν_8 shows up in both $A_{1g} + 4E_g$ and T_{2g} polarizations, in accordance with light scattering selection rules for molecular librations in cubic crystals[6] and with the triple-approach model. In addition, this is the only mode to show different x dependences at ambient and low temperatures (see Fig. 6 and 7), a property that is connected to the low-temperature orientational glass state.

The localized excitation ν_8 was first recognized in the INS work mentioned previously for a series of alkali halides with low NH_4^+ content ($x < 5\%$).[9] In particular, for a 4.5% ammonium concentration diluted in KI, a value of 230 cm^{-1} was found at $T = 80$ K. Owing to the broad INS feature, the agreement with the data of Table III for the low-impurity limit is satisfactory.

Librational transitions of molecular impurities are of interest since their corresponding energies enable us to derive the potential barriers hindering the reorientations. For that, the local symmetry of the crystal field acting on NH_4^+

in KI has to be assumed. As mentioned in Sec. I, there are now reliable hints in favor of the triple approach model.[8] Within this picture, one N–H bond points towards one of the eight equivalent C_3 axes.

Using ν_8 data from Tables II and III, we have calculated the barrier heights $V(x,T)$ according to the simple harmonic approximation[9]

$$V(x,T) = \frac{8\pi^2 I_{am}}{n^2}\,\nu_8\,(x,T)^2; \qquad (1)$$

where I_{am} denotes the moment of inertia of the protonated ammonium molecule [$I_{am} = 4.8\times10^{-47}$ kg m^2 (Ref. 9)]. The periodicity n of the barrier is related to the angular separation between two C_3 axis directions, namely, 70.5°, so that we take $n = 5.1$ (360/70.5).[21] The variation of the hindering barriers with the NH_4^+ composition is displayed in Fig. 10 for the four samples considered. Data for the deuterated crystal [$x(D) = 0.42$] have been omitted. It remains, however, unclear why there is no isotope effect on ν_8, while according to Eq. (1), the ND_4^+ libration should occur at much lower frequency (diminished by a factor 1.4 assuming identical V and n) than in the hydrogenated system.

As for the librational frequencies, Fig. 10 reveals two different behaviors: At room temperature the 20% decrease in the activation energies observed as x passes from 0.5% to 46% is partly due to the augmentation of the lattice parameter in the mixed crystal ($x\to1$).[2,6] On the contrary, at $T = 7$ K, $V(x)$ increases slightly. These different features can be simply understood in terms of NH_4^+–NH_4^+ electric dipolar interactions. In the paraelectric plastic phase, the ammonium ions rotate almost freely, so that the dipolar interactions between molecules are averaged to zero. In the orientational glassy state, these interactions are frozen and thus act as an additional potential which increases the energy barrier against reorientations. This qualitative analysis is supported by a neutron study of the NH_4^+-tunneling transitions in KI:NH_4I (Ref. 2).

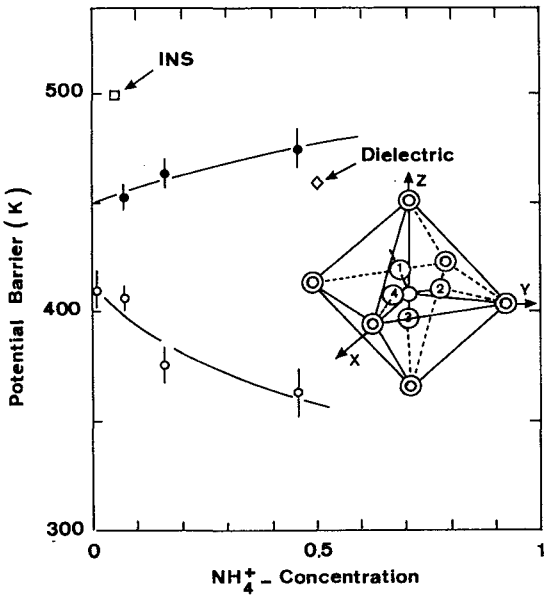

FIG. 10. Variation of the barrier heights $V(x)$ deduced from the NH_4^+ libration ν_8, [Eq. (1)] as function of ammonium concentration. Closed circles: $T = 7$ K, open circles: $T = 295$ K. Data points labeled INS and dielectric are from Refs. 9 and 4, respectively. Continuous curves are a guide for the eyes only. Inset: preferential orientations of the ammonium molecule in f.c.c. according to the triple-approach model.

Although we are aware that we provide a simple quantitative analysis of the rotational excitations in $K_{1-x}(NH_4)_xI$, it is worthwhile comparing the present results on potential barriers with those of previous works. If one extrapolates the results of Fig. 10 to the end members KI and NH_4I, one gets for room temperature values 410 and ~300 K, respectively. At 7 K, in the impurity limit, $V(x\to0) \simeq 450$ K.

(i) At ambient temperature first, $V(x = 1)$ can be compared to the NMR results in the cubic plastic phase reported by Sharp and Pintar:[22] from the Arrhenius behaviour of the spin lattice relaxation time, they deduced for ND_4I an activation energy of 380 K.

(ii) On the other side of the phase diagram and for $T = 2$ K, Bostoen *et al.*[2] derived from the analysis of the tunneling splitting levels of isolated NH_4^+ molecules in KI a value $V(x\to0) = 285$ K.

(iii) A recent determination of the hindering barrier in $K_{0.57}(NH_4)_{0.43}I$ was provided from a frequency analysis of the freezing process using dielectric measurements. The value of 460 K was obtained.

Owing to the variety of experimental determinations of the barrier heights in $K_{1-x}(NH_4)_xI$, the Raman data in Fig. 10 show an overall good agreement with the values mentioned above.

Very recently, Tomkinson *et al.* have extended their INS measurements to the $K_{1-x}(NH_4)_xI$ family up to $x = 62\%$.[21] These authors observed a contribution to the INS spectra ($T = 20$ K) arising from rotational localized excitations. However, contrary to the $x = 4.5\%$ data published previously,[9] this rotational band is revealed at much higher energy, in the range 250–260 cm^{-1}. Moreover, in contradiction with the present Raman data they found a band position which decreases with increasing mole fraction (see Fig. 10 for comparison).

IV. CONCLUDING REMARKS

For a series of potassium ammonium iodide mixed crystals, we have presented low-energy Raman scattering measurements at ambient and low temperature ($T = 7$ K).

In these systems the substitution $K^+ \to NH_4^+$ for $x \lesssim 0.50$ prevents the occurence of the structural phase transitions typical for pure ammonium halides. This property enabled us to observe at low temperatures the Raman contributions of translational and rotational modes in a NaCl-type cubic phase, where the NH_4^+ reorientations are assumed to be frozen in.

In both plastic and frozen phases, the orientational disorder lifts the wave vector conservation of the Raman scattering processes, and thus phonon modes of the whole Brillouin zone contribute to the light scattering spectrum. At room temperature, however, these excitations are consider-

ably broadened through the dynamical orientational disorder.

Below 250 cm^{-1}, seven Raman active components could be identified in $K_{1-x}(NH_4)_xI$. Three modes at $\simeq 30$, $\simeq 50$, and 60 cm^{-1} have been assigned to density of states of acoustic phonons. At higher frequency, two components, around 80 and 170 cm^{-1} arise from impurity modes related to ammonium molecules diluted in pure KI. At 110 cm^{-1}, the observed Raman band results most probably from optical phonons already present in potassium iodide.

In addition, we have observed in all compounds a mode of libration of the NH_4^+ molecules at $\simeq 220$ cm^{-1}. The energy of this rotational excitation was used to estimate the potential barrier hindering the NH_4^+ reorientations.

In order to test the dynamical properties of the NH_4^+ freezing process we plan to extend the present investigation to higher composition ($x \geqslant 0.5$) and to the whole temperature range $T = 4$ to 300 K.

ACKNOWLEDGMENT

We are indebted to Dr. Guiraud for his analysis of the ammonium contents in $K_{1-x}(NH_4)_xI$ crystals.

[1] N. G. Parsonage and L. A. K. Staveley, *Disorder in Crystals* (Oxford University, Oxford, 1978).
[2] C. Bostoen, G. Coddens, and W. Wegener, J. Chem. Phys. **91**, 6337 (1989). Claude Bostoen, Ph.D., University of Antwerpen, Belgium, 1991 (unpublished).
[3] J.-F. Berret, F. Bruchhäuser, R. Feile, C. Bostoen, and S. Haussühl, Solid State Commun. **74**, 1041 (1990).
[4] I. Fehst, R. Böhmer, W. Ott, A. Loidl, S. Haussühl, and C. Bostoen, Phys. Rev. Lett. **64**, 3139 (1990).
[5] W. Joosen, H. Fleurent, C. Bostoen, D. Schoemaker, and S. Haussühl, Phys. Rev. B **43**, 11542 (1990).
[6] J.-F. Berret, C. Bostoen, J.-L. Sauvajol, B. Hennion, and S. Haussühl, Europhys. Lett. **16**, 91 (1991).
[7] I. Fehst, S. L. Hutton, R. Böhmer, A. Loidl, and S. Haussühl, Proceedings of the 7th European Meeting on Ferroelectricity, Dijon 1991.
[8] Y. Ozaki, K. Maki, K. Okada, and J. A. Morrison, J. Phys. Soc. Jpn. **54**, 2595 (1985); Y. Ozaki, *ibid.* **56**, 1017 (1987).
[9] A. B. Gardner, T. C. Waddington, and J Tomkinson, J. Chem. Soc. Faraday Trans. 2 **73**, 1191 (1977).
[10] A. Heidemann, J. Howard, K. J. Lushingston, J. A. Morrison, W. Press, and J. Tomkinson, J. Phys. Soc. Jpn. **52**, 2401 (1983).
[11] W. Dultz and H. Ihlefeld, J. Chem. Phys. **58**, 3365 (1973).
[12] M. Couzi, J. B. Sokoloff, and C. H. Perry, J. Chem. Phys. **58**, 2965 (1973).
[13] H. D. Hochheimer, E. Spanner, and D. Strauch, J. Chem. Phys. **64**, 1583 (1976). H. D. Hochheimer, M. L. Shand, C. T. Walker, and A. Huller, *Ibid.* **71**, 5008 (1979).
[14] T. Schräder, A. Loidl, and T. Vogt, Phys. Rev. B **39**, 6186 (1989).
[15] J.-F. Berret, J.-L. Sauvajol, and G. Cohen-Solal, Europhys. Lett. **13**, 273 (1990), and references therein.
[16] J.-F. Berret, C. Bostoen, J.-L. Sauvajol, and B. Hennion (to be published, 1992).
[17] L. Genzel and W. Bauhofer, Z. Phys. B **28**, 13 (1976).
[18] J. H. Fertel and C. H. Perry, Phys. Rev. **184**, 874 (1969).
[19] G. Dolling, R. A. Cowley, C. Schittenhelm, and I. M. Thorson, Phys. Rev. **147**, 577 (1966).
[20] N. Vagelatos, J. M. Rowe, and J. J. Rush, Phys. Rev. B **12**, 4522 (1975).
[21] J. Tomkinson, B. A. Dasannacharya, P. S. Goyal, and R Chakravarthy, J. Chem. Soc. Faraday Trans. **87** (1991).
[22] A. R. Sharp and M. M. Pintar, J. Chem. Phys. **53**, 2428 (1970).